PHYSICAL REVIEW A, VOLUME 62, 012505

Spectroscopic characterization of the ZnNe van der Waals molecule in the $X0^+(4\ ^1S_0)$ and $D1(4\ ^1P_1)$ energy states

J. Koperski* and M. Czajkowski†
Department of Physics, University of Windsor, Windsor, Ontario, Canada N9B 3P4

(Received 21 December 1998; revised manuscript received 8 October 1999; published 8 June 2000)

A molecular jet-expansion beam of ZnNe seeded in Ne was crossed with a pulsed-laser beam produced by a Nd:YAG (yttrium aluminum garnet) laser-pumped dye laser. The dye laser was frequency doubled with a BBO-C second-harmonic-generation (SHG) crystal. Both the dye laser and the SHG were synchronously scanned over a range of $\lambda = 2130-2170$ Å in the vicinity of the Zn atomic $4\ ^1P_1 - 4\ ^1S_0$ resonance line (2138.65 Å), producing an excitation spectrum related to the $D1(4\ ^1P_1) \leftarrow X0^+(4\ ^1S_0)$ transition in the ZnNe molecule. The spectral traces, which show a pronounced vibrational structure, were subjected to LeRoy's near-dissociation expansion (NDE) analysis, yielding ω_e, $\omega_e x_e$, D_e, and long-range molecular potential parameters. Computer simulation of the excitation spectrum, based on a calculation of the Franck-Condon factors, yielded additional information on the equilibrium internuclear separation for the $D1$ and $X0^+$ states. The NDE analysis provided long-range characteristics for the $X0^+$ state of the CdNe and HgNe molecules as well. A simple dispersive model, and a combination rule for van der Waals interactions in the ground state of ZnNe, CdNe, and HgNe molecules, are discussed.

PACS number(s): 33.20.Lg, 33.20.Tp, 33.15.Fm

I. INTRODUCTION

A precise knowledge of the potential-energy (PE) curves of diatomic molecules is of primary interest for understanding basic quantum-mechanical phenomena such as collisional energy transfer, recombination and scattering processes, chemical reactivity involving excited states, line broadening phenomena, atom- (or molecule-) surface interaction, and many others. On the other hand, the most direct way to investigate experimentally such interactions between two electrically neutral atoms and/or molecules and, consequently, to obtain precise information on the interaction potentials, seems to be (in most cases) the utilization of modern methods of laser spectroscopy (in various forms) combined with jet-expansion atomic (molecular-) beam techniques [1]. These methods allow one to observe emission and/or absorption spectra related to even very weakly bound species which are known under the common name of van der Waals (vdW) molecules (or clusters) [2]. The last decade showed an avalanche of papers on the subject of molecules which can be generally described as MRG diatomic clusters. Here M stands for a metal atom (e.g., Na, K, Zn, Cd, Hg, etc.), and RG represents a rare-gas atom (He, Ne, Ar, Kr, and Xe). The combination of such atoms forms a truly vdW molecule which represents the most simple theoretical example of an induced-dipole–induced-dipole-type interaction. Consequently, some very interesting studies have been performed on systems such as NaRG [3,4], HgRG [5–9], CdRG [10–15], and AgRG [16,17], and quite recently on ZnRG [18–20]. In reality, all these molecules do not exist under ordinary laboratory conditions of normal temperature and pressure. Due to their very weak bonding they dissociate rapidly when colliding with other atomic (molecular) partners. Therefore, they can be investigated only under extremely demanding conditions of low temperature and a very low number of collisions with environmental partners. Indeed, all the experimental work mentioned above utilized supersonic beam methods to form and to observe the vdW molecules. The experimental results provide a full spectroscopic characterization of the molecules in their excited states and possibly their ground states. Consequently, the main features of the forces responsible for molecule formation and its persistence in ground or excited states can be evaluated from the spectra, and they can be further compared with theoretical predictions of quantum mechanical calculations (see e.g., Refs. [21–23]).

At present, ZnRG molecules are the subject of extensive investigation as the last kind of unobserved vdW molecules consisting of a IIb-group M atom and a RG partner. The most recent work has been reported by Breckenridge and co-workers on ZnAr, ZnKr, and ZnXe [18–20]. They provided spectroscopic potential parameters for the $D1(4\ ^1P_1)$ molecular state and, to a lesser extent, attempted to describe the $X0^+(4\ ^1S_0)$ ground state of the molecules. Furthermore, Czajkowski and Koperski reported on ZnAr and ZnKr complexes, presenting more details regarding the ground state of these molecules. Preliminary results on the subject were presented at the TWICOLS'95 and EGAS'96 international conferences, and published in the conference proceedings [24,25].

In our present work we report on the excitation spectra of the $D1(4\ ^1P_1) \leftarrow X0^+(4\ ^1S_0)$ transition in ZnNe molecules observed in a supersonic beam seeded in a cold environment of Ne. Figure 1 illustrates the PE curves drawn for the $X0^+$ ground state and $D1$ excited state. ZnNe is a very simple

---

*Permanent address: Instytut Fizyki, Uniwersytet Jagielloński, ul. Reymonta 4, 30-059 Kraków, Poland.
Electronic address: ufkopers@cyf-kr.edu.pl

†Author to whom correspondence should be addressed. Electronic address: mczajko@uwindsor.ca

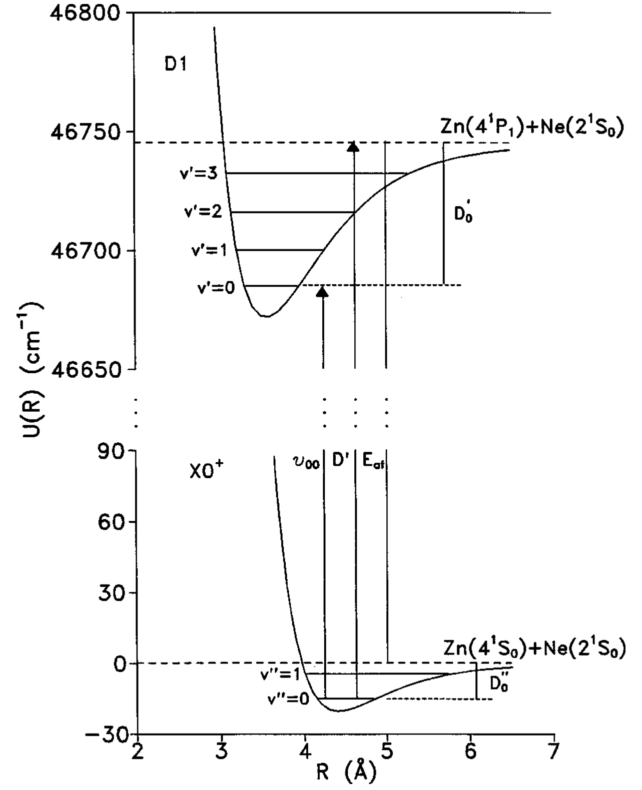

FIG. 1. Potential-energy curves for the ZnNe molecule in the $X0^+(4\ ^1S_0)$ ground state and the $D1(4\ ^1P_1)$ excited state. The curves are drawn according to the experimental molecular parameters using a simple Morse approximation. Depicted are one of the observed transitions, ν_{00}, as well as the dissociation energies of the excited and ground states, D_0' and D_0'', the dissociation limit of the excited state, D', and the energy corresponding to the $4\ ^1P_1$–$4\ ^1S_0$ atomic transition, $E_{\rm at}$.

molecule which, to the best of our knowledge, has no record in the scientific literature (see the Note added in proof). We have observed the vibrational spectra of this complex at different temperatures of the beam, and, hence, we obtained some ‘‘hot’’ vibrational bands, which provided direct information on the ground state of the molecule. LeRoy's near-dissociation-expansion (NDE) analysis as well as theoretical calculation of the Franck-Condon (FC) factors [26] enabled us to obtain spectroscopic potential parameters of ZnNe in $D1$ and $X0^+$ states.

II. EXPERIMENT

The arrangement of the apparatus is shown in Fig. 2. Laser-induced fluorescence (LIF) was observed in an evacuated expansion chamber into which the Zn atoms seeded in neon were injected through a nozzle (150 μm in diameter, D) constituting part of the molecular-beam source made of a solid molybdenum. This material, in spite of the fact that it is very difficult to machine, is essential for production of ZnNe molecules in their ground state by means of thermal source. Metallic zinc at high temperature (920–1020 K) is chemically very active with other metals, which may be used to fabricate the source [27]. A stainless-steel source, for instance, which we have used before [28], began to corrode soon after the oven reached 870 K. The fine nozzle would be damaged severely and eventually clogged in a short time after a relatively high saturated vapor pressure of zinc is established in the source. Conversely, the molybdenum source keeps the nozzle clear for many hours, and the source can be recharged many times over. Some details of the thermal source fabrication were described previously [28].

The ZnNe vdW molecules in the beam were irradiated with a second-harmonic output of an in-house-built dye laser utilizing a $7.0\times10^{-4}\ M/L$ solution of Coumarin 460 in di-

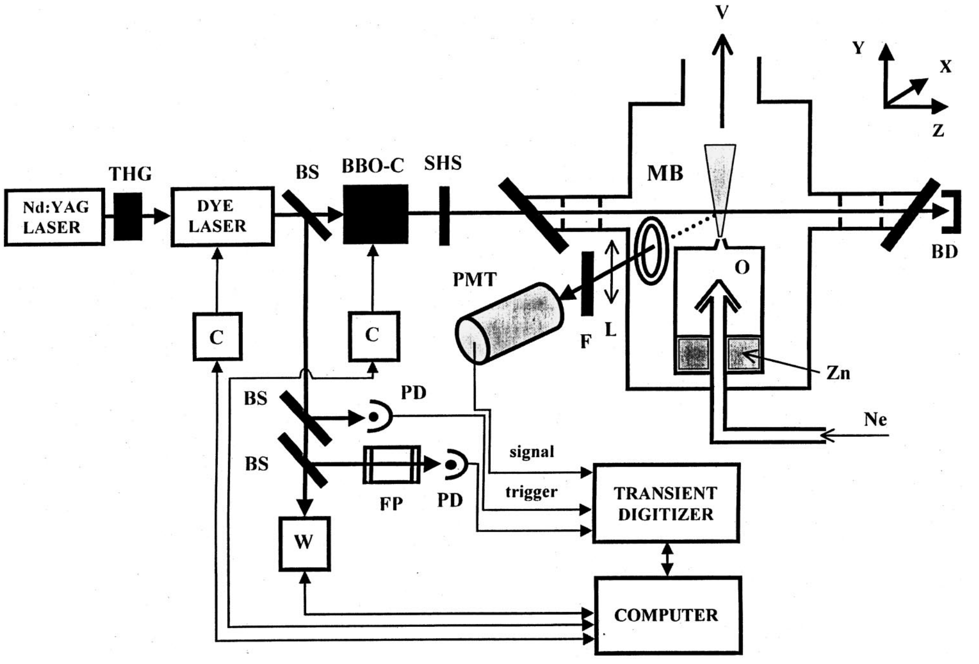

FIG. 2. Schematic diagram of the apparatus. THG, third harmonic generator of the Nd:YAG laser frequency. BS, beam splitter. BBO-C, dye-laser frequency doubling crystal. SHS, second-harmonic separator. FP, Fabry-Perot interferometer. MB, molecular beam. O, oven. V, vacuum pump system. BD, laser beam dump. L lens. F, filter. PMT, photomultiplier tube. W, wave meter. C, scanning control device. PD, photodiode.

methyl sulphoxide pumped with the third-harmonic output of a Q-switched Nd:YAG (yttrium aluminum garnet) laser. A BBO-C frequency doubling crystal used in conjunction with the dye laser was scanned by a computer simultaneously with the dye laser over the range of $\lambda = 2130-2170$ Å. The wavelength calibration of the dye laser was frequently verified against a Fizeau-wedge wave meter (W) [29]. The spectral line width of the dye laser output, monitored with a Fabry-Perot etalon, was found to be approximately 1.5–2.0 cm^{-1}.

The resulting excitation spectrum was monitored at a right angle to the plane containing the crossed molecular and laser beams, and detected with a Schlumberger EMR-541-N-03-14 photomultiplier tube (PMT) with its peak sensitivity in the UV and blue spectral response regions. In fact, the PMT was practically insensitive to wavelengths longer than $\lambda \approx 6200$ Å. Additionally, a narrow band filter (F) with $\Delta\lambda = 100$ Å (half width at half maximum) centered at $\lambda = 2140$ Å was placed in front of the PMT to reject stray light and improve the signal-to-noise ratio. The PMT signal was recorded with a transient digitizer (Hewlett-Packard, model HP54510A Digitizing Oscilloscope) and stored in a computer.

The beam source was operated at a temperature of about $T_{\mathrm{oven}} = 920-950$ K, which corresponded to a Zn-saturated vapor pressure of about 50 torr. The carrier gas backing pressure P_0 was maintained in the range from 10 to 14 atm while the X/D parameter ratio was varied from 27 to 64, where X is a distance measured from the nozzle to the laser beam (excitation region). Thus the excitation distance X was varied from 4.0 to 9.6 mm. This permitted observations of the LIF in different regions of the supersonic beam corresponding to different conditions of temperature and appropriate number of collisions between the ZnNe molecules and the carrier gas atoms [30]. Successively, we observed some ''hot'' vibrational bands produced in $v'(=0,1,2) \leftarrow v''(=1)$ of the $D1(4\ ^1P_1) \leftarrow X0^+(4\ ^1S_0)$ transition. We also found that at lower Ne pressures an insufficient number of ZnNe molecules was produced, while a further increase of the distance $X(X > 10\ \mathrm{mm})$, which might improve the cooling efficiency [30], resulted in a rapid decline of the LIF signal as the density of the molecules in the beam decreased. On the whole, the mechanical and thermal stability of the apparatus was very satisfactory, as was the reproducibility of the spectra.

III. RESULTS AND ANALYSIS OF THE SPECTROSCOPIC DATA

The excitation spectrum of the $D1(4\ ^1P_1) \leftarrow X0^+(4\ ^1S_0)$ transition of ZnNe is shown in Fig. 3. The vibrational bands are located very close to the $4\ ^1P_1 \leftarrow 4\ ^1S_0$ atomic transition, and the entire spectrum spans a range of approximately 3 Å, which in this spectral region corresponds to about 65 cm^{-1}. Excitation spectra were recorded for several values of the X/D ratio. Results for $X/D = 27$, 40, and 54, shown in Fig. 3, are labeled (a), (b), and (c), respectively. Hot bands originating from $v'' = 1$ are evident in the spectra recorded with $X/D = 27$ and 40. The pronounced vibrational band with the longest wavelength [see trace (c)] has been assigned to the fundamental $v' = 0 \leftarrow v'' = 0$ transition. This is similar to our observation of the CdNe excitation spectrum [31]. Some fluorescence measurements and a computer simulation of the spectrum confirmed this assignment. The frequencies of the vibrational bands in the $D1 \leftarrow X0^+$ band system are collected in Table I.

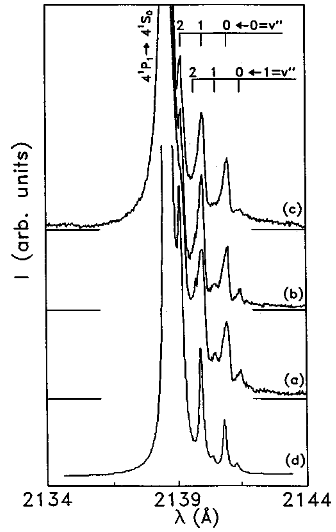

FIG. 3. $D1(4\ ^1P_1) \leftarrow X0^+(4\ ^1S_0)$ excitation spectra of the ZnNe molecule recorded for (a) $X/D = 27$, (b) $X/D = 40$, and (c) $X/D = 54$ parameters. $D = 150\ \mu$m, $T_{\mathrm{oven}} = 920$ K, and $P_0 \approx 10$ atm. (d) Theoretical simulation of the total $D1 \leftarrow X0^+$ excitation spectrum. A FWHM of 2.2 cm^{-1} was used for the Lorentzian convolution function.

A. Near-dissociation theory analysis

1. $X0^+(4\ ^1S_0)$ state

Table I also lists the experimental frequencies of the ''hot'' bands observed in the $D1 \leftarrow X0^+$ transition of ZnNe. From ''cold'' and ''hot'' progressions the first vibrational spacing in the ground state was estimated to be $\Delta G(\frac{1}{2}) = 9.8 \pm 0.4\ \mathrm{cm}^{-1}$. It is known [32,33] that for very weakly bound vdW systems a Morse-type linear Birge-Sponer (BS) extrapolation [34] is not adequate to describe the long-range behavior of the internuclear potential. As the dissociation limit is approached, the vibrational spacings $\Delta G(v'' + 1/2)$ depend mainly on the asymptotically dominant inverse-power contribution to the interatomic potential,

$$U(R) \simeq D'' - \frac{C_n}{R^n}, \tag{1}$$

with an appropriate exponent n to describe the dominant long-range interactions present, where D'' is the ground-state dissociation limit (here equal to D_0''), and C_n is a constant. For the ZnNe ground state, the long-range interaction between Zn and Ne atomic closed shells (with $4s^2$ and $2p^6$ symmetries, respectively) is purely vdW in nature [i.e., $n = 6$ in Eq. (1)], and the dispersion coefficient C_6'' provides the dominant contribution to the binding. Since the highest

TABLE I. Energies of the $D1 \leftarrow X0^+$ transitions of the ZnNe molecule. *Using the GVNDE program (see text).

	ν (cm^{-1})		
$v' \leftarrow v''$	Experimental	Calculated*	$\Delta G(v'+1/2)$
$0 \leftarrow 0$	46698.7 ± 0.2	-	
			20.5 ± 0.4
$1 \leftarrow 0$	46719.2 ± 0.2	-	
			16.4 ± 0.4
$2 \leftarrow 0$	46735.6 ± 0.2	-	
			12.2 ± 0.2
$3 \leftarrow 0$	-	46747.79	
			8.10
$4 \leftarrow 0$	-	46755.89	
			4.37
$5 \leftarrow 0$	-	46760.26	
			1.67
$6 \leftarrow 0$	-	46761.93	
			0.26
$7 \leftarrow 0$	-	46762.19	
''Hot'' bands			
$0 \leftarrow 1$	46688.9 ± 0.2	-	-
$1 \leftarrow 1$	46709.4 ± 0.3	-	-
$2 \leftarrow 1$	46724.7 ± 0.5	-	-
$\nu = \nu_1(v' \leftarrow v''=0) - \nu_2(v' \leftarrow v''=1) = 9.8 \pm 0.4$ cm^{-1}			

observed vibrational spacing for the ground state is much smaller than that for the $D1$ state, and because a reasonably good C_6'' can be estimated from theory (see below), we started our analysis from a determination of the ground-state properties. When the close-to-dissociation vibrational levels are measured experimentally, it is advisable to employ the limiting near-dissociation procedure of LeRoy and Bernstein (LRB) [35], especially when a plausible estimate of the limiting C_6'' coefficient can be generated. In situations like the present one, with no close-to-dissociation experimental evidence, it is recommended to apply a recently developed generalized NDE method, and use the GVNDE program of Le Roy and co-workers [36,37] for fitting vibrational energies to the NDE. The program allows one to determine the long-range potential characteristics (i.e., D'' or v_D'', the effective vibrational quantum number at dissociation) even when the close-to-dissociation limit vibrational transitions are not measured. It was successfully applied in many cases [36–38], and proved itself to be a very good tool that supplements the limiting near-dissociation LRB procedure. In Ref. [37] the author provided a detailed description of the procedure for fitting vibrational-level energies to the NDE. Here we present only a general idea of the method.

The generalized NDE procedure is based on the equation (written for ground-state characteristics).

$$E_{v''} = D'' - X_0(n)(v_D'' - v'')^{2n/(n-2)} f(v_D'' - v''), \qquad (2)$$

where $E_{v''}$ is an energy of the ground-state vibrational level v'', $X_0(n) = \widetilde{X}_0(n)/[\mu^n (C_n)^2]^{1/(n-2)}$, μ is a reduced mass of the ZnNe molecule (in amu), $\widetilde{X}_0(n)$ is a known numerical factor depending only on physical constants and the value of n [35,36,39], and the $f(v_D'' - v'')$ term is some empirically determined analytic function which is constrained to approach 1 as v'' approaches v_D''. In the GVNDE program the $f(v_D'' - v'')$ term is represented by a ratio of polynomials in $f(v_D'' - v'')$. Equation (2) incorporates the limiting behavior of the limiting near-dissociation procedure [i.e., Eq. (2) without the $f(v_D'' - v'')$] into empirical expansions that account for the observed pattern of energies of the *lower* vibrational levels v''. The program performs fits to a variety of these $f(v_D'' - v'')$ forms, and generates weighted averages of the physically significant parameters (D'', v_D'', or C_n). This eventually yields more realistic estimates of these parameters that could otherwise be obtained. In particular, it replaces unrestrained empirical extrapolation by an interpolation between experimental data for levels lying far from the dissociation limit, and the exactly known functional behavior at the limit. This known limit behavior is introduced into the program by the plausible estimate of the leading C_n, coefficient and hence the program gives a more realistic extrapolation.

As already stated above, in the case of the ZnNe ground state the dominant inverse-power term in the long-range intermolecular potential corresponds to an R^{-6} term. A plausible estimate for the C_6'' coefficient could be evaluated with the help of a Slater-Kirkwood [40] formula: $C_6'' = 3\alpha_{\mathrm{Zn}}\alpha_{\mathrm{Ne}}/2[(\alpha_{\mathrm{Zn}}/N_{\mathrm{Zn}})^{1/2} + (\alpha_{\mathrm{Ne}}/N_{\mathrm{Ne}})^{1/2}]$, where α_{Zn} and α_{Ne} are static polarizabilities (in a.u.) in their ground electronic states, and N_{Zn} and N_{Ne} are numbers of electrons in the outer shell of Zn and Ne atoms, respectively. To evaluate C_6'' (ZnNe), we used $\alpha_{\mathrm{Ne}} = 2.67$ a.u. [41] and a recently published value for the static polarizability of Zn atom $\alpha_{\mathrm{Zn}} = 38.8 \pm 0.8$ a.u. [42,43]. We obtained $C_6''(\mathrm{ZnNe}) = 31.2$ a.u. (i.e., 0.150×10^6 cm^{-1}Å^6), and this value was used in the GVNDE program. With average atomic masses of Zn and Ne atoms and a first vibrational spacing in the ground state $\Delta G(1/2)$, the program generated the effective vibrational index at the dissociation limit $v_D'' = 3.58 \pm 0.30$ and the dissociation limit for the ZnNe ground state $D'' = D_0'' = 16.8 \pm 1.2$ cm^{-1}, as well as other characteristics of the $X0^+$ state (i.e., ω_e'', $\omega_e'' x_e''$, and D_e'') and remaining energies of the ground-state vibrational levels $E_{v''=2} = 14.90$ cm^1 and $E_{v''=3} = 16.64$ cm^1. The $X0^+$-state potential parameters are collected in Table II.

2. *D1(4 $^1P_1$) state*

Having determined the ground-state characteristics, one considers a simple relationship

$$E_{\mathrm{at}} + D_0'' = \nu_{00} + D_0' = D', \qquad (3)$$

where D_0' is the $D1$-state dissociation energy, and E_{at} and ν_{00} are energies corresponding to the 4 $^1P_1$-4 $^1S_0$ atomic and $D1(v'=0) \leftarrow X0^+(v''=0)$ transitions, respectively (see

TABLE II. Molecular constants for the ZnNe $X0^+$ and $D1$ states.

Designation	$X0^+$	$D1$
D_0 (cm^{-1})	16.8 ± 1.2[a] 20[c]	63.6 ± 1.0[a]; 63.5 ± 1.4[b] 69[c]
ω_e (cm^{-1})	15.06 ± 1.8[a] 15 ± 3[c]	25.35 ± 1.07[a]; 24.6[d] 25.8 ± 0.4[c]
$\omega_e x_e$ (cm^{-1})	2.68 ± 0.9[a] 2.1[c]	2.99 ± 0.89[a]; 2.05[d] 2.34 ± 0.2[c]
D_e (cm^{-1})	23.6 ± 1.2[a] 27[c]	75.53 ± 1.00[a]; 73.8[e] 81[c]
v_D	3.58 ± 0.30[a]	$7.08-7.43\pm0.31$[a]
R_e (Å)	4.42 ± 0.06[f] 4.16 ± 0.10[c]	3.58 ± 0.08[g] 3.48 ± 0.06[c]
$\Delta R_e = R_e' - R_e''$ (Å)	-0.85 ± 0.02[h]	
T_{vib} (K)	~8.0[h]	

[a] From a GVNDE program for generalized near-dissociation expansion (recommended values).

[b] From Eq. (3).

[c] Reference [61] (see Note added in proof).

[d] From a Birge-Sponer extrapolation.

[e] From the $D_e' \approx (\omega_e')^2/4\omega_e' x_e'$ approximation.

[f] Estimated from the D_e'' and α_{RG} correlation (Luiti and Pirani method).

[g] Estimated using R_e'' and the best fit of ΔR_e.

[h] From the best fit of the simulated excitation spectra for $v' \leftarrow v'' = 0$ and $v' \leftarrow v'' = 1$ transitions.

Fig. 1). Using Eq. (3) we calculated the excited-state properties $D_0' = 63.5\pm1.4\,\text{cm}^{-1}$ and $D' = 46762.2\pm1.4\,\text{cm}^{-1}$. As the first three transitions in the $v' \leftarrow v'' = 0$ progression were measured we attempted to characterize a close-to-equilibrium region of the $D1$-state potential well with the help of a Morse-type linear BS extrapolation [ΔG vs $(v' + \frac{1}{2})$ plot]. From the BS plot we evaluated ω_0' (a short extrapolation, i.e., an intercept with the vertical axis) and $\omega_0' x_0' \approx \omega_e' x_e'$ (a slope) values, and then a $\omega_e' \approx \omega_0' + \omega_0' x_0'$ value which characterizes the potential only in the vicinity of R_e'. To describe the long-range part of the potential we employed the GVNDE program to fit the $D1$-state vibrational levels near the dissociation. As input parameters we used the experimentally measured $E_{v'}$ energies of the $v' = 0,1,2 \leftarrow v'' = 0$ transitions (see Table I). While an accurate $C_6'(D1)$ is not readily available for this state, the fact that the limiting near dissociation theory coefficient depends on a fractional power of C_6' means that the uncertainty in its value should not affect the extrapolation too much. The constant $C_6'(D1)$ should be significantly larger than $C_6''(X0^+)$, and a factor of 2 difference seems plausible. We varied the $C_6'(D1)$ estimate in the program within the range of $0.2-0.4\times10^6\,\text{cm}^{-1}\,\text{Å}^6$, and with D' fixed at the value determined above the program generated $E_{v'}$ values up to dissociation, as well as the effective vibrational index at the dissociation limit, v_D' and other $D1$-state characteristics. The ΔG vs $(v' + \frac{1}{2})$ plot shown in Fig. 4 presents a comparison between results of both BS and general NDE methods. It illustrates that the $D1$-state dissociation energy, D_0', and v_D' would be underestimated if determined with the BS plot. Therefore, the characteristics obtained using the GVNDE program are the recommended values from this study as they take into account the fact that the nature of the long-range behavior of the potential provides the dominant contribution to the bonding. The results are collected in Tables I and II.

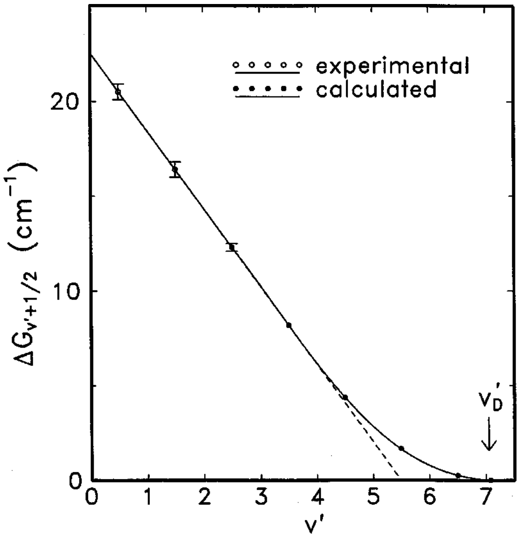

FIG. 4. ΔG vs $(v' + \frac{1}{2})$ plot for the v' progression in the $D1 \leftarrow X0^+$ spectrum of ZnNe. Experimental and generated (using the GVNDE program) points are indicated (also see Table I). The effective vibrational index at the dissociation limit, v_D', obtained from the general NDE theory, is depicted. The plot illustrates an inadequacy of using the BS method to determine true value for the $D1$-state dissociation energy and v_D' (underestimation). Error bars for the experimental points are shown.

3. Simulation of the excitation spectrum

The simulation of the excitation spectrum provided some additional information on the ground- and excited-state parameters. The simulation employed a computer program [26] designed to calculate the FC factors, based on an assumption that both initial and final states are well represented by a Morse potential. The result of the simulation is shown in Fig. 5. Next to the $v' \leftarrow v'' = 0$ progression (thick bars) the simulation also includes the ''hot'' band, $v' \leftarrow v'' = 1$ progression (thin bars). The ''best'' simulated spectrum required the vibrational temperature of $T_{\text{vib}} \approx 8$ K. Then, having determined all the FC factors, we simulated the total $D1(v') \leftarrow X0^+(v'' = 0,1)$ spectrum. The experimental trace was quite well reproduced assuming that the laser is represented by a Lorentzian convolution function with a width of 2.2-cm^{-1} full width at half maximum (FWHM), a conclusion which agrees with our earlier experimental determination. The result of the total simulation is shown in Fig. 3(d), and should be compared with the experimental trace of Fig. 3(c).

The main reason to perform the simulation of the total spectrum was to obtain a value for the difference $\Delta R_e = R_e' - R_e''$ of the equilibrium internuclear separation in the excited (R_e') and ground (R_e'') states. It has been found that ΔR_e

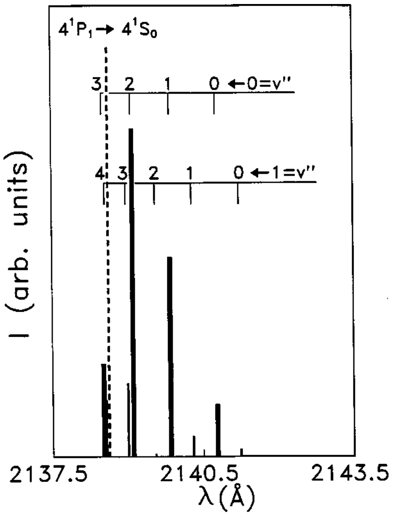

FIG. 5. Computer simulation of the ZnNe $D1 \leftarrow X0^+$ excitation spectrum for $v' \leftarrow v'' = 0$ (thick bars) and $v' \leftarrow v'' = 1$ hot (thin bars), progressions. Morse potentials were assumed for both states; $\Delta R_e = R_e' - R_e'' = -0.85 \pm 0.02$ Å, and $T_{\mathrm{vib}} \approx 8$ K was obtained as a result of the simulation (‘‘best fit’’).

$= -0.85 \pm 0.02$ Å, indicating that the minimum of the PE curve of the excited state is shifted by 0.85 Å toward the shorter equilibrium distance with respect to the location of the ground-state minimum. This is supported by the fact that the experimental profiles of the vibrational bands are ‘‘shaded’’ toward blue. It should be mentioned here that we did not attempted to reproduce the blue shading of the vibrational bands. Our intention was to show an influence of the neighboring atomic line, which is large in amplitude, and apparently affects the intensity distribution among particular vibrational bands.

B. Estimation of R_e'' of the ZnNe molecule

Liuti and Pirani [44] found some useful regularities related to the vdW interactions. They discovered a correlation between the potential parameters and atomic polarizabilities which leads, as a consequence, to a correlation of the C_6 constants describing the long-range interaction to the potential well depth D_e and equilibrium distance R_e. References [44] and [45] cite about 50 systems (among them MRG complexes) for which the correlation works with a remarkable accuracy, assuming that the long-range forces are in operation only. We applied this correlation to our system to estimate R_e'' in the ZnNe molecule:

$$R_e''(\mathrm{MRG}) = \left[\frac{D_e''(\mathrm{ref})}{D_e''(\mathrm{MRG})}\right]^{1/6} \left[\frac{C_6''(\mathrm{MRG})}{C_6''(\mathrm{ref})}\right]^{1/6} R_e''(\mathrm{ref}), \quad (4)$$

where $R_e''(\mathrm{MRG})$ is the equilibrium distance of the investigated MRG molecule; $R_e''(\mathrm{ref})$ is the equilibrium distance of a ‘‘reference’’ ref molecule; $D_e''(\mathrm{MRG})$ and $D_e''(\mathrm{ref})$ are the dissociation energies of the investigated and reference molecules, respectively; and $C_6''(\mathrm{MRG})$ and $C_6''(\mathrm{ref})$ are the long-range coefficient (C_6/R^6) of the investigated and reference molecules, respectively. As suggested in Ref. [44] the C_6'' values were evaluated using the Slater-Kirkwood formula [40]. In our estimation of $R_e''(\mathrm{ZnNe})$ we employed seven reference (ref) molecules: CdNe [11], HgNe [5], NaNe [3], MgNe [46], ZnAr [18], CdAr [11,47], and HgAr [5]. We used accurately measured values of the equilibrium internuclear separations $R_e''(\mathrm{ref})$ (from analysis of rotationally resolved spectra) and dissociation energies $D_e''(\mathrm{ref})$ that were reported for these molecules, as well as the $D_e''(\mathrm{ZnNe}) = 23.6\ \mathrm{cm}^{-1}$ obtained in our experiment. For Cd and Hg atomic polarizabilities, as for Zn, we used recently published values: $\alpha_{\mathrm{Cd}} = 49.7 \pm 1.6$ a.u. [43,48] and $\alpha_{\mathrm{Hg}} = 33.9 \pm 0.3$ a.u. [43,49], that are known with higher accuracy than those of Refs. [41,50]. As the result of the numerical estimation [Eq. (4)] we obtained $R_e''(\mathrm{ZnNe}) = 4.42 \pm 0.06$ Å. Next, using $\Delta R_e = -0.85 \pm 0.02$ Å, we obtained the $R_e' = 3.58 \pm 0.08$ Å for the excited $D1$ state. Both results seem to be very reasonable as compared to the sizes of the molecules in the CdRG and HgRG families [51,5–7,9,11–13]. We included these values in Table II.

IV. DISCUSSION AND CONCLUSIONS

A. ZnNe, CdNe, and HgNe families of molecules

Table III summarizes some potential parameters determined in this study for the ZnNe molecule in the ground $X0^+$ state and excited $D1$ state. For comparison, the molecular parameters of CdNe and HgNe in the same molecular states are included as well. Additionally, assuming that the ground states of the CdNe and HgNe molecules in the long-range approximation are also governed by a pure vdW interaction, we applied the GVNDE program to determine $D'' = D_0''(\mathrm{CdNe})$, $D'' = D_0''(\mathrm{HgNe})$, $v_D''(\mathrm{CdNe})$, and $v_D''(\mathrm{HgNe})$, as we did for the ZnNe molecule. As input parameters we used known $\nu = \nu_1(v' \leftarrow v'' = 0) - \nu_2(v' \leftarrow v'' = 1)$ separations [7,31,52], and plausible estimates of C_6'' obtained using the Slater-Kirkwood formula. An interesting experimental trend can be observed. The binding energies of the ground state increase in the sequence: $D_e''(\mathrm{HgNe}) > D_e''(\mathrm{CdNe}) > D_e''(\mathrm{ZnNe})$. This trend in binding energies is similar as in analogous MAr, MKr, and MXe ($M = \mathrm{Zn, Cd, Hg}$) complexes [47,51]. However, the MNe complexes considered here are very simple, and are bound only by dispersive forces which can be treated quantitatively using models, e.g., like those proposed by London [53] and Drude [54]. According to these models the dispersive interaction between M and Ne atoms is expressed by $U_{M\mathrm{Ne}} = -C_6/R^6$, where $C_6 = 3 I_M I_{\mathrm{Ne}} \alpha_M \alpha_{\mathrm{Ne}} / 2(I_M + I_{\mathrm{Ne}}) = 3F^{-1} \alpha_M \alpha_{\mathrm{Ne}}/2$, I_M and I_{Ne} are approximated by the ionization potentials of atoms M and Ne, and α_M and α_{Ne} are their respective static polarizabilities. Cited in Table III are the polarizabilities of Zn, Cd, and Hg, which were taken from Refs. [41–43,48–50]. However, the values of atomic polarizabilities of Zn, Cd, and Hg do not exhibit any particular trend which may be responsible for any influence on the interaction energy. In fact, their values are close to each other (see $\alpha_M^{(\mathrm{Tab})}$ in Table III), and so are the reduced ionization potentials F related to ZnNe, CdNe, and HgNe molecules. Contrary to this, the binding energies

TABLE III. Potential parameters of the ZnNe, CdNe, and HgNe in the $X0^+$ and $D1$ states.

	ZnNe		CdNe		HgNe	
Potential parameter	$X0^+$	$D1$	$X0^+$	$D1^{a}$	$X0^+$	$D1^{b}$
D_e (cm^{-1})	23.6^{c}; (20.3)^{d,e}	73.0	28.3^{a}; (31.4)^{c}	76.0	42.0^{f}; (44.2)^{c}	94.7
R_e (Å)	4.42	3.58	4.30^{a}; 4.20^{f}	3.54	3.90^{f}	3.41
$\alpha_{Me}^{(\mathrm{Tab})}$ (Å^3)	5.6^{g}; 5.7^{h}	-	6.0^{g}; 7.2^{i}; 7.3^{h}	-	5.7^{g}; 5.1^{h}	-
F^{-1}[1/(cm^{-1})]^{j}	52 757	-	51 171	-	56 692	-
$''\times 10^{-6}$ (cm^{-1} Å^6)	0.150^{k}; 0.178^{e}	-	0.172^{k}; 0.222^{e}	-	0.141^{k}; 0.172^{e}	-

[a] References [31,52].
[b] Reference [60].
[c] From the GVNDE program (this work).
[d] From the Birge-Sponer approximation (previous studies).
[e] London-Drude model, and Refs. [24,25].
[f] Reference [7].
[g] Reference [50].
[h] References [42,43,48,49].
[i] Reference [41].
[j] Reference [59].
[k] From the Slater-Kirkwood formula (see text).

which should be proportional to the C_6'' parameters, indicate a well-defined increase running from 23.6 cm^{-1} for ZnNe, to 31.4 cm^{-1} for CdNe, and finally reaching 44.2 cm^{-1} for HgNe (as obtained in a long-range approximation using the GVNDE program). Following a suggestion of Ref. [55], and particularly one of Ref. [56] and the London-Drude model, this observed trend can be explained qualitatively in a simple manner by assuming a *steric effect* [55], which relates to differences in electron charge density of the s^2 shell in M atoms. In the sequence of Zn:Cd:Hg atoms their atomic radii calculated as a half distance of closest approach of atomic centres in the crystalline state are 1.33 Å: 1.48 Å: 1.56 Å [41], respectively. Assuming a simple picture of spherical interacting atoms, it is possible that two neutral atoms like Zn and Ne may establish an equilibrium distance of interaction which would be effectively longer that the one established by the same Ne atom and larger Hg atoms. This apparently surprising conclusion may be a result of the different electron charge of the outer s^2 shell of M atoms. The Ne atom may partially penetrate the outer ns^2 shells; therefore, the penetration is more effective in the case of the Hg($6s^2$) outer shell than in case of the Zn($4s^2$) shell. Under such an assumption this is a result of the effective difference in the $'e^- \text{-} e^-'$ repulsive interaction of the outer electrons of both atoms. At this point it is worthwhile to mention that the bond lengths of the discussed molecules also change, decreasing from $R_e''(\mathrm{ZnNe}) = 4.42$ Å, through $R_e''(\mathrm{CdNe}) = 4.27$ Å, to $R_e''(\mathrm{HgNe}) = 3.90$ Å (see Table III), that supports the general model described above.

B. Unobserved $A0^+(4\ ^3P_1) \leftarrow X0^+(4\ ^1S_0)$ and $B1(4\ ^3P_1) \leftarrow X0^+(4\ ^1S_0)$ transitions

Some interesting although unwanted effects may be observed in a supersonic beam if the excited species have an abnormally large lifetime in the excited state. This is the case of ZnRG molecules when they are excited to the $A0^+(4\ ^3P_1)$ and $B1(4\ ^3P_1)$ states. The length of the lifetime τ can be conveniently converted into a distance (L) which an excited atom or molecule travels in the beam with the speed of the gas flow. If L is large enough then the molecule traveling along the straight line path (without radiation) may easily leave the ''region of visibility'' of the detection system. The region of visibility is defined by the geometry of the experiment, but it is usually limited by means of a set of optical baffles as a protection against scattered light. Therefore, due to the specifics of the jet-expansion beam [30], the excited molecule may vanish completely from the observation window, later being deactivated rapidly by collisions. If we consider a specific case of ZnNe and employ theoretical considerations, notation, and formulas of Ref. [30], we can obtain a very instructive numerical conclusion. For $P_0 = 10$ atm of Ne, $T_T \approx 2$ K (the translational temperature in the beam), using $\tau(\mathrm{Zn}\ 4\ ^3P_1) = 27\ \mu$s [57], and $X/D = 53$, we calculated the ''terminal distance'' X_T (the location of the ''Mach disk'') and the distance L to be 1.3 and 4.7 cm, respectively. Since the ''Mach disk'' is the limit of the so-called ''zone of silence'' in the jet-expansion beam, this means that the excited molecule will enter the region of high-temperature chaos and dissociate rapidly due to extensive collision processes. This phenomenon may be one of the possible explanation why the normally visible triplet asymptotic $A0^+(n\ ^3P_1)$ and $B1(n\ ^3P_1)$ (with $n = 5$ and 6 for CdNe and HgNe, respectively) is not observed in case of ZnRG molecules ($n = 4$) [18]. Here we excluded any relation of this failure to a lack of the detection sensitivity of our experimental systems as a possible cause.

Another possibility, which is so far purely speculative, may be related to an ''abnormally'' large $\Delta R_e = R_e' - R_e''$, the difference in the equilibrium positions of the excited and ground states of ZnRG, which makes the bound-state excitation process impossible for Franck-Condon reasons. Since both of the lowest excited states seem to be inaccessible for excitation, then we have to assume that ΔR_e is too large for the $A0^+$ state ($R_e' < R_e''$), and too small for the $B1$ state ($R_e' > R_e''$). Such a requirement appears to be too much of a coincidence, since the whole family of five different molecules (ZnRG) must exhibit such anomalous behavior. Thus, in our opinion, the former explanation is more plausible, bearing in mind a very small oscillator strength of the $4\ ^3P_1 - 4\ ^1S_0$ atomic transition which plays the main role in defining the values of probabilities of the molecular transitions, as it was shown in the case of a CdAr molecule [58]. An experiment is prepared in our laboratory to make the observation geometry of the instrumental setup most favorable for excited molecules to be detected at a long distance away from the nozzle and, hence, to observe the excitation spectra of the $A0^+ \leftarrow X0^+$ and $B1 \leftarrow X0^+$ transitions.

V. CONCLUSIONS

We report an observation (see the Note added in proof) of the ZnNe excitation spectrum of the $D1(4\ ^1P_1) \leftarrow X0^+(4\ ^1S_0)$ transition. We analyzed the spectrum including several ''hot'' bands, and evaluated the potential parameters for the molecule in its $D1$ and $X0^+$ states. Long-range characteristics by means of LeRoy's near-dissociation expansion (NDE) analysis have been determined. Simulation of the excitation spectrum yielded information on the equilibrium internuclear separation for the excited and ground states. The NDE analysis also provided long-range characteristics for the $X0^+$ state of the CdNe and HgNe molecules. Ground-state C_6'' parameters for the MNe (M = Zn, Cd, and Hg) molecules were generated using a simple combination rule for vdW interaction.

Note added. Recently an article of McCaffrey *et al.* [61] on the spectroscopic characterization of ZnNe $^1\Sigma^+$ and $^1\Pi_1$ vdW states was published. Partially resolved rotational spectra presented there allowed for excited-state characterization and (since ''hot'' bands were not observed) for an indirect ground-state characterization. Spectroscopic characteristics of the ground and excited states obtained in Ref. [61] are collected in Table II for comparison.

ACKNOWLEDGMENTS

This research was supported by a grant from the Natural Science and Engineering Research Council of Canada. One of us (J.K.) was partially supported by the Polish State Committee for Scientific Research (K.B.N.), Grant No. 2 P03B 107 10. We would like to express our gratitude to Professor Robert J. LeRoy of the University of Waterloo, Ont., Canada for his GVNDE program, as well as for his help in its application.

[1] *Atomic and Molecular Beam Methods*, edited by G. Scoles (Oxford University Press, London, 1988), Vol. 1.

[2] B. L. Blaney and G. E. Ewing, Annu. Rev. Phys. Chem. **27**, 553 (1976).

[3] M. P. Lapatovich, R. Ahmed-Bitar, P. E. Moskovitz, I. Renhorn, R. A. Gottscho, and D. A. Pritchard, J. Chem. Phys. **73**, 5419 (1980); J. Tellinghuisen, A. Ragone, M. Soo Kim, D. J. Auerbach, R. E. Smalley, L. Wharton, and D. H. Levy, J. Chem. Phys. **71**, 1283 (1979).

[4] R. E. Smalley, D. A. Auerbach, P. S. H. Fitch, D. H. Levy, and L. Wharton, J. Chem. Phys. **66**, 3778 (1977).

[5] K. Yamanouchi, J. Fukuyama, H. Horiguchi, S. Tsuchiya, K. Fuke, T. Saito, and K. Kaya, J. Chem. Phys. **85**, 1806 (1986); K. Fuke, T. Saito, and K. Kaya, *ibid.* **81**, 2591 (1984); K. Yamanouchi, S. Isogai, N. Okunischi, and S. Tsuchiya, *ibid.* **88**, 205 (1988); T. Tsuchizawa, K. Yamanouchi, and S. Tsuchiya, *ibid.* **89**, 4646 (1988).

[6] N. Okunishi, K. Yamanouchi, H. Nakazawa, and S. Tsuchiya, J. Chem. Phys. **93**, 7526 (1990).

[7] J. Koperski, J. B. Atkinson, and L. Krause, Chem. Phys. **186**, 401 (1994).

[8] R. D. van Zee, S. C. Blankespoor, and T. S. Zwier, Chem. Phys. Lett. **158**, 306 (1989).

[9] J. Koperski, Chem. Phys. **211**, 191 (1996); **214**, 431 (1997).

[10] A. Kowalski, M. Czajkowski, and W. H. Breckenridge, Chem. Phys. Lett. **121**, 217 (1985).

[11] A. Kvaran, D. J. Funk, A. Kowalski, and W. H. Breckenridge, J. Chem. Phys. **89**, 6069 (1989).

[12] R. Bobkowski, M. Czajkowski, and L. Krause, Phys. Rev. A **41**, 243 (1990).

[13] M. Czajkowski, R. Bobkowski, and L. Krause, Phys. Rev. A **44**, 5730 (1991).

[14] M. Czajkowski, R. Bobkowski, and L. Krause, Phys. Rev. A **45**, 6451 (1992).

[15] J. Koperski and M. Czajkowski, J. Chem. Phys. **109**, 459 (1998).

[16] L. R. Brock and M. A. Duncan, J. Chem. Phys. **103**, 9200 (1995).

[17] K. F. Willey, P. Y. Cheng, C. S. Yeh, D. L. Robbins, and M. A. Duncan, J. Chem. Phys. **95**, 6249 (1991).

[18] I. Wallace, R. R. Bennett, and W. H. Breckenridge, Chem. Phys. Lett. **153**, 127 (1988).

[19] R. R. Bennett and W. H. Breckenridge, J. Chem. Phys. **92**, 1588 (1989).

[20] I. Wallace, J. G. Kaup, and W. H. Breckenridge, J. Phys. Chem. **95**, 8060 (1991); I. Wallace, J. Rytter, W. H. Breckenridge, J. Chem. Phys. **92**, 1588 (1989).

[21] E. Czuchaj and J. Sienkiewicz, J. Phys. B **17**, 2251 (1984).

[22] E. Czuchaj, H. Stoll, and H. Preuss, J. Phys. B **20**, 1487 (1987).

[23] E. Czuchaj and J. Sienkiewicz (private communication).

[24] M. Czajkowski and J. Koperski, in *Laser Spectroscopy XII International Conference*, edited by M. Inguscio, M. Allegrini, and A. Sasso (World Scientific, Singapore, 1996), pp. 392–393.

[25] M. Czajkowski and J. Koperski, in *EGAS 26th International Conference, Graz 1996, Europhysics Conference Abstract*, edited by L. Windholz (EPS, Geneva, 1988), pp. 19–20; Koperski and M. Czajkowski, *ibid.* pp. 551–552.

[26] J. Supronowicz (private communication).

[27] R. Burman (unpublished).

[28] M. Czajkowski, R. Bobkowski, and L. Krause, Phys. Rev. A **41**, 277 (1990).

[29] W. Kedzierski, R. W. Berends, J. B. Atkinson, and L. Krause, J. Phys. Sci. Instrum. **21**, 796 (1988).

[30] L. B. Lubman, C. T. Rettner, and R. N. Zare, J. Phys. Chem. **86**, 1129 (1982).

[31] J. Koperski and M. Czajkowski, Eur. Phys. J. D (to be published).
[32] R. J. LeRoy, J. Chem. Phys. **57**, 573 (1972).
[33] Y. Tanaka, K. Yoshino, and D. E. Freeman, J. Chem. Phys. **59**, 5160 (1973).
[34] R. T. Birge and H. Sponer, Phys. Rev. **28**, 259 (1926).
[35] R. J. Le Roy and R. B. Bernstein, J. Chem. Phys. **52**, 3869 (1970); Chem. Phys. Lett. **5**, 42 (1970).
[36] R. J. Le Roy and W.-H. Lam, Chem. Phys. Lett. **71**, 544 (1980).
[37] R. J. Le Roy, J. Chem. Phys. **101**, 10 217 (1994).
[38] J. W. Tromp and R. J. Le Roy, J. Mol. Spectrosc. **109**, 352 (1985); K. J. Jordan, R. H. Lipson, N. A. McDonald, and R. J. Le Roy, J. Phys. Chem. **96**, 4778 (1992).
[39] R. J. LeRoy, in *Semiclassical Methods in Molecular Scattering and Spectroscopy*, edited by M. S. Child (Reidel, Dordrecht, 1980), p. 109.
[40] J. C. Slater and J. G. Kirkwood, Phys. Rev. **37**, 682 (1931).
[41] *Science Data Book*, edited by R. M. Tennent (Oliver & Boyd, Edinburgh, 1976).
[42] D. Goebel, U. Hohm, and G. Maroulis, Phys. Rev. A **54**, 1973 (1996).
[43] M. Yu and M. Dolg, Chem. Phys. Lett. **273**, 329 (1997); M. Seth, P. Schwerdtfeger, and M. Dolg, J. Chem. Phys. **106**, 3623 (1997).
[44] G. Liuti and F. Pirani, Chem. Phys. Lett. **122**, 1245 (1985).
[45] R. Cambi, D. Cappelletti, G. Liuti, and F. Pirani, J. Chem. Phys. **95**, 1852 (1991).
[46] I. Wallace and W. H. Breckenridge, J. Chem. Phys. **98**, 2768 (1993).
[47] D. J. Funk, A. Kvaran, and W. H. Breckenridge, J. Chem. Phys. **90**, 2915 (1989).
[48] D. Goebel and U. Hohm, Phys. Rev. A **52**, 3691 (1995).
[49] D. Goebel and U. Hohm, J. Phys. Chem. **100**, 7710 (1996).
[50] M. M. Miller and B. Bederson, Adv. At. Mol. Phys. **13**, 1 (1977).
[51] W. H. Breckenridge, C. Jouvet, and B. Soep, in *Advances in Metal and Semiconductor Clusters*, edited by M. Duncan (JAI, Greenwich, 1995), Vol. 3, pp. 1–83.
[52] M. Czajkowski, L. Krause, and R. Bobkowski, Phys. Rev. A **49**, 775 (1994).
[53] F. London, Z. Phys. **63**, 243 (1930); Z. Phys. Chem. Abt. B **11**, 222 (1930).
[54] G. C. Maitland, M. Rigby, E. B. Smith, and W. A. Wakeham, *Intermolecular Forces* (Clarendon, Oxford, 1987).
[55] C. Jouvet, C. Lardeux-Dedonder, S. Martrenchard, and D. Solgadi, J. Chem. Phys. **94**, 1759 (1991).
[56] J. Wallace, J. Ryter, and W. H. Breckenridge, J. Chem. Phys. **96**, 136 (1992).
[57] M. Czajkowski, R. Bobkowski, and L. Krause, Spectrochim. Acta B **46**, 1161 (1991).
[58] M. Czajkowski, R. Bobkowski, and L. Krause, Phys. Rev. A **40**, 4338 (1989).
[59] *Atomic Energy Levels*, edited by C. E. Moore, Natl. Bur. Stand. U.S. NSRDS No. 35 (U.S. GPO, Washington, DC, 1971).
[60] T. Tsuchizawa, K. Yamanouchi, and S. Tsuchiya, J. Chem. Phys. **89**, 4646 (1988).
[61] J. G. McCaffrey, D. Bellert, A. W. K. Leung, and W. H. Breckenridge, Chem. Phys. Lett. **302**, 113 (1999).